

Mechanistic Study of Cu-Mediated,
Photoinduced C–S Bond Formation
and Demonstration of Electrochemical
Ammonia Production by a Surface-
Attached Iron Complex

Thesis by
Kareem Imad Hannoun

In Partial Fulfillment of the Requirements for
the degree of
Doctor of Philosophy

Caltech

CALIFORNIA INSTITUTE OF TECHNOLOGY
Pasadena, California

2019
(Defended May 6, 2019)

ACKNOWLEDGEMENTS

My time at Caltech has been both fulfilling and frustrating. I have been privileged to work with an incredible group of scientists, from whom I have learned and grown immensely. As an advisor, Jonas has given me this opportunity and challenged me to grow as a scientist and person. The other members of my committee have also encouraged me to achieve more and provided support and guidance along the way. I especially have to thank the members of the Peters lab I've had the honor of overlapping, who have helped me in more ways than I could possibly list here. I especially have to thank Yichen Tan, Jon Rittle, and John Anderson, who all helped me get on my feet in a new environment. Miles Johnson was a great colleague who really pushed me to do thorough and careful science and had a lasting influence on the way I approach my work self-critically.

I would also like to thank the training and mentorship I received as an undergraduate. Richard Jordan took me in as a clueless undergraduate and showed great patience with me as I acquired the skills and knowledge necessary to succeed. His fastidiousness and kind feedback encouraged me to continue in chemistry and develop a keen eye for data analysis. The camaraderie I experienced in the Jordan group gave me an opportunity to learn from many scientists with disparate backgrounds.

I need to thank all the friends who've helped me through graduate school. Nik Thompson and Blake Daniels were instrumental in my happiness and adjustment to Caltech. Paul Walton, Trevor Del Castillo, Ben Matson, and Mark Nesbit have all provided great experiences, from hiking and camping together to roasting coffee. Nina Gu has supported me over the past couple of years and provided constant friendship and willingness to have

new experiences outside of lab. Michael McGovern has been a consistent source of support and encouragement. Although we don't get to talk or see each other as often as we would like, I know he's always there for me.

Last, but not least, I need to thank my family for their unwavering support and belief. My parents and my sister Deena have always been encouraging during difficult stretches and I'm lucky to have such a loving family who support me unwaveringly.

ABSTRACT

The worldwide reliance on fossil fuels for energy and petrochemicals poses a massive environmental hazard. Furthermore, many chemical processes rely on precious metals that have low abundance on Earth and are threatened. As the world population grows rapidly, these factors pose an increasing threat to our planet and new chemical processes are needed that employ earth-abundant catalysts and alternative chemical currencies such as light and electricity derived from renewable sources.

Chapter 2 discusses an in-depth mechanistic study of the photoinduced, copper-mediated cross-coupling of aryl thiols with aryl halides. This reaction employs light energy and an earth-abundant metal to achieve bond formation through a pathway distinct from that of thermal reactions. In particular, I focus on the stoichiometric photochemistry and subsequent reactivity of a $[\text{Cu}^{\text{I}}(\text{SAr})_2]^-$ complex (Ar = 2,6-dimethylphenyl). A broad array of experimental techniques furnish data consistent with a pathway in which a photoexcited $[\text{Cu}^{\text{I}}(\text{SAr})_2]^{-*}$ complex undergoes SET to generate a Cu^{II} species and an aryl radical, which then couple through an in-cage radical recombination.

Chapter 3 discusses the surface attachment of a $\text{P}_3^{\text{B}}\text{Fe}$ complex to a carbon electrode, and the electrochemical generation of ammonia from N_2 by the surface-appended species ($\text{P}_3^{\text{B}}\text{Fe}$ = tris-phosphinoborane). Ammonia production is achieved industrially by the combination of N_2 and H_2 , the latter of which is derived from methane with concomitant production of CO_2 . Alternative chemical processes, such as the use of energy derived from electricity, are vital for the decreasing the carbon footprint of ammonia production. Synthetic modification of a previously-reported $\text{P}_3^{\text{B}}\text{Fe}$ complex by addition of three pyrene substituents onto the catalyst backbone allows non-covalent attachment onto a graphite surface. The

resulting functionalized electrode shows good stability towards iron desorption under highly reducing conditions, and produces 1.4 equiv NH_3 per iron site. The data presented provide the first demonstration of electrochemical nitrogen fixation by a molecular complex appended to an electrode.

PUBLISHED CONTENT AND CONTRIBUTIONS

- (1) Johnson, M. W.[†]; **Hannoun, K. I.**[†]; Tan, Y.; Fu, G. C.; Peters, J. C. A Mechanistic Investigation of the Photoinduced, Copper-Mediated Cross-Coupling of an Aryl Thiol with an Aryl Halide. *Chem. Sci.* **2016**, *7* (7), 4091–4100. <https://doi.org/10.1039/C5SC04709A>. K.I.H. participated in running experiments, data analysis, DFT calculations, and manuscript preparation.

[†]These authors contributed equally.

TABLE OF CONTENTS

Acknowledgements	iii
Abstract	v
Published Content and Contributions.....	vii
Table of Contents.....	viii
List of Illustrations and/or Tables	x
Nomenclature.....	xiii
Chapter I: Introduction	1
1.1 Motivation	1
1.2 Copper-Mediated Cross Coupling and Photochemistry.....	2
1.3 Mechanism of Copper-mediated Coupling Reactions	3
1.4 Reduction of N ₂ to NH ₃ by Molecular Catalysts.....	6
1.5 Surface Attachment of Molecular Electrocatalysts	10
1.6 Chapter Summaries	12
1.7 References	13
Chapter II: A Mechanistic Investigation of Photoinduced, Copper-Catalyzed Cross-Couplings of Aryl Thiols with Aryl Halides.....	21
2.1 Introduction	21
2.2 Results and Discussion.....	23
2.3 Conclusions	43
2.4 References	45
Chapter III: Electrochemical Ammonia Production by a Surface-Attached Iron Complex	55
3.1 Introduction	55
3.2 Results and Discussion.....	56
3.3 Conclusion	62
3.4 References	62
Appendix A: Supplementary Information for Chapter II.....	66
A.1 General Considerations	66
A.2 Synthesis and Characterization	70
A.3 Molar Conductivity Measurements	76
A.4 Spectroscopic Identification of Copper(II) Species	76
A.5 Identification of 2.1 by ESI-MS.....	77
A.6 Radical Clock Experiments.....	78
A.7 Stoichiometric of [Cu ^I (SAr) ₂]Na with Phenyl Halides	81
A.8 Stern-Volmer Quenching Experiment	81
A.9 Steady-State Fluorimetry Experiment	82
A.10 Reactivity of 1-(but-3-en-1-yloxy)-2-iodobenzene with [Cu ^I (SAr) ₂]Na.....	82
A.11 VT-NMR Study of 2.1	83
A.12 DOSY Experiment	83
A.13 Actinometric Studies	84

A.14 Emission Spectrum of 100-W Hg Lamp	86
A.15 Absorption Spectra of 2.1 in the Presence of 2.2	88
A.16 DFT Calculations	89
A.17 Probe of Direct Coupling between [Cu ^I (SAr) ₂]Na (2.1) and Aryl Radical ..	92
A.18 X-Ray Crystallographic Data.....	96
A.19 ¹ H and ¹³ C NMR Data.....	97
A.20 References.....	110
Appendix B: Supplementary Information for Chapter III.....	113
B.1 General Considerations.....	113
B.2 Synthesis and Characterization	115
B.3 Chemical Ammonia Generation Experiments	119
B.4 Electrochemistry	119
B.5 Electrochemical Ammonia Generation Experiments.	123
B.6 Electrode Desorption Experiment	124
B.7 Supplementary XPS data.....	125
B.8 NMR Spectra	125
B.9 References.....	129

LIST OF ILLUSTRATIONS AND TABLES

Chapter I:	
Scheme 1.1: Copper-mediated Ullmann coupling	2
Scheme 1.2: Copper-catalyzed, ligand-accelerated Ullmann coupling	3
Figure 1.1 Photoexcitation of a Cu ^I -amide to access a highly reducing excited state and photoinduced C–N cross-coupling catalyzed by a Cu ^I -amide	3
Figure 1.2: Possible pathways for ligand-accelerated Ullmann coupling reactions	4
Figure 1.3: Radical clock experiments disfavoring the intermediacy of an aryl radical in the copper-catalyzed C–N and C–S coupling reactions.....	5
Scheme 1.3: Model chemistry demonstrating the viability of a Cu ^I /Cu ^{III} cycle based on oxidative addition and reductive elimination for C–N coupling	5
Figure 1.4: Early mechanistic studies of photoinduced, Cu-catalyzed cross-coupling.....	6
Figure 1.5: First examples of N ₂ activation and catalytic reduction	8
Figure 1.6: Electrochemical reduction of N ₂	9
Figure 1.7: Overview of common strategies for surface attachment of molecular electrocatalysts	11
Chapter II:	
Equation 2.1	21
Equation 2.2	22
Figure 2.1: Outline of a possible catalytic cycle for photoinduced, copper-catalyzed cross-coupling.....	22
Equation 2.3	23
Figure 2.2: An alternative mechanism: coupling of an aryl radical with a copper(I)-thiolate as a key step.....	24
Figure 2.3: An alternative mechanism: S _{RN1}	25
Figure 2.4: An alternative mechanism: concerted oxidative addition	25
Equation 2.4	26
Equation 2.5	27
Equation 2.6	27
Figure 2.5: X-ray crystal structure of [Cu ^I (SAr) ₂][Na(12-crown-4) ₂] (2.1).....	28
Equation 2.7	29
Figure 2.6: Cyclic voltammograms of [Cu ^I (SAr) ₂ Na (2.1) and of NaSAr.....	30
Figure 2.7: Optical spectrum and time-resolved luminescence of 2.1	32
Figure 2.8: Difference density plot for the lowest energy absorption band of [Cu ^I (SAr) ₂ Na (2.1).....	33
Figure 2.9: Stern–Volmer plot for the luminescence quenching of [Cu ^I (SAr) ₂ Na* in the presence of Ph–I.....	34
Equation 2.8.....	35
Table 2.1: Reactions of a copper–thiolate with an aryldiazonium salt	36

Equation 2.9	36
Table 2.2: Reaction of an aryl radical: Cyclization versus capture by a copper–thiolate	38
Equation 2.10	39
Figure 2.10: X-band EPR spectrum (77 K) of a coupling reaction following irradiation for 5 min	40
Figure 2.11: Optical spectrum of a coupling reaction prior to photolysis and after photolysis in propionitrile at $-78\text{ }^{\circ}\text{C}$	41
Equation 2.11	41
Equation 2.12	42
Figure 2.12: Spin density plots of $[\text{Cu}^{\text{II}}(\text{SAr})_3]^-$ and $\text{Cu}^{\text{II}}(\text{SAr})_2$	43
Chapter III:	
Scheme 3.1	57
Scheme 3.2	57
Figure 3.1: UV-vis spectra of authentic sample of 3.3 and sample of 3.3 recovered from functionalized electrode	59
Figure 3.2: Cyclic voltammograms of functionalized and unfunctionalized electrodes	60
Table 3.1: Yields of NH_3 from CPE experiments with $\text{P}^{\text{v}}\text{P}_3^{\text{B}}\text{FeMe}$ -functionalized electrodes	61
Figure 3.3: XPS spectra	62
Appendix A:	
Figure A.1: Representative example of reaction setup using a 100-W Hg lamp ...	69
Table A.1: Molar conductivities of measured compounds	76
Figure A.2: ESI-MS of 2.1	78
Table A.2: Reactivity of 2.1 with 1-(allyloxy)-2-iodobenzene	79
Table A.3: Reactivity of 2.1 with 1-(but-3-en-1-yloxy)-2-iodobenzene	80
Table A.4: Reactivity of 2.1 with 2-iodobenzophenone	80
Table A.5: Stability of radical clocks	80
Table A.6: Reactivity of 2.1 with iodobenzene and control experiments	81
Table A.7: Excited-state lifetime as a function of quencher concentration	82
Table A.8: Product distribution in the reaction of 2.1 with 1-(but-3-en-1-yloxy)-2-iodobenzene	82
Figure A.3: Low temperature and ambient temperature ^1H NMR of 2.1	83
Table A.9: Measured hydrodynamic radii	84
Table A.10: DFT-calculated radii	84
Figure A.4: Emission spectrum of 100-W Blak-Ray Long Wave Ultraviolet Lamp (Hg)	87
Figure A.5: Absorbance spectra of $[\text{Cu}^{\text{I}}(\text{SAr})_2]\text{Na}$ in acetonitrile at various concentrations	87
Figure A.6: Absorbance spectra of sodium 2,6-dimethylthiophenolate in acetonitrile at various concentrations	88
Figure A.7: Optical spectra of 2.1 in the presence of increasing concentrations of sodium 2,6-dimethylthiophenolate	88
Figure A.8: Optical spectra of 2.1 in the presence of	

sodium 2,6-dimethylthiophenolate at variable temperature.....	89
Figure A.9: Calculated free energies of two possible Cu(I) speciations.....	90
Figure A.10: Calculated free energies of three possible Cu(II) speciations	90
Table A.11: Free energies of computed molecules	90
Figure A.11: Spin density plots of Cu(2,6-dimethylthiophenolate) ₂ and [Cu(2,6-dimethylthiophenolate) ₃] ⁻	91
Figure A.12: DFT structures of Cu(2,6-dimethylthiophenolate) ₂ and [Cu(2,6-dimethylthiophenolate) ₃] ⁻ showing the orientation of the g tensor ...	92
Table A.12: Crystal Data and Structure Refinement for 2.1	96
Figure A.13: ¹ H NMR of [Cu ^I (SAr) ₂ Na].....	97
Figure A.14: ¹ H NMR of Sodium 2,6-dimethylthiophenolate.....	98
Figure A.15: ¹ H NMR of 4-Methoxyphenyl 2,6-dimethylphenyl sulfide	99
Figure A.16: ¹³ C NMR of 4-Methoxyphenyl 2,6-dimethylphenyl sulfide	100
Figure A.17: ¹ H NMR of 2-(Allyloxy) 2,6-dimethylphenyl sulfide.....	101
Figure A.18: ¹³ C NMR of 2-(Allyloxy) 2,6-dimethylphenyl sulfide.....	102
Figure A.19: ¹ H NMR of 3-(2,6-dimethylphenylthiomethyl)-2,3-dihydrobenzo-furan.....	103
Figure A.20: ¹³ C NMR of 3-(2,6-dimethylphenylthiomethyl)-2,3-dihydrobenzo-furan.....	104
Figure A.21: ¹ H NMR of 2-(2,6-dimethylphenylthio)-benzophenone	105
Figure A.22: ¹³ C NMR of 2-(2,6-dimethylphenylthio)-benzophenone	106
Figure A.23: ¹ H NMR of 2-(but-3-en-yloxy) 2,6-dimethylphenyl sulfide	107
Figure A.24: ¹³ C NMR of 2-(but-3-en-yloxy) 2,6-dimethylphenyl sulfide.....	108
Figure A.25: ¹ H NMR of 4-(methylchromane) 2,6-dimethylphenyl sulfide.....	109
Figure A.26: ¹³ C NMR of 4-(methylchromane) 2,6-dimethylphenyl sulfide.....	110
Appendix B:	
Figure B.1: Cyclic voltammogram of ^{py} P ₃ ^B (3.1).....	121
Figure B.2: Cyclic voltammogram of ^{py} P ₃ ^B FeMe (3.3)	121
Figure B.3: Cyclic voltammogram of [^{py} P ₃ ^B FeN ₂][Na(THF) _n] (3.4)	122
Figure B.4: Cyclic voltammograms of surface-attached ^{py} P ₃ ^B (3.1).....	123
Figure B.5: Overview XPS spectra.....	125
Figure B.6: ¹ H NMR of 3-Iodo-4-Bromo- <i>O</i> -(1-pyrenyl-butyl)phenol	125
Figure B.7: ¹³ C{ ¹ H} NMR of 3-Iodo-4-Bromo- <i>O</i> -(1-pyrenyl-butyl)phenol	126
Figure B.8: ¹ H NMR of 3-diisopropylphosphino-4-Bromo- <i>O</i> -(1-pyrenyl-butyl)phenol	126
Figure B.9: ³¹ P{ ¹ H} NMR of 3-diisopropylphosphino-4-Bromo- <i>O</i> -(1-pyrenyl-butyl)phenol	126
Figure B.10: ¹ H NMR of ^{py} P ₃ ^B (3.1).....	127
Figure B.11: ³¹ P{ ¹ H} NMR of ^{py} P ₃ ^B (3.1)	127
Figure B.12: ¹ H NMR of ^{py} P ₃ ^B FeBr (3.2).....	127
Figure B.13: ¹ H NMR of ^{py} P ₃ ^B FeMe (3.3)	128
Figure B.14: ¹ H NMR of [^{py} P ₃ ^B FeN ₂][Na(THF) _n] (3.4).....	128

NOMENCLATURE

- A.** Absorbance.
Å. Angstrom.
Ar. Aryl group.
ATR. Attenuated Total Reflectance.
A(X). Hyperfine coupling constant due to nucleus X
BAr^F₄. [B(3,5-C₆H₃(CF₃)₂)₄]⁻
Carb. Carbazolide.
Cat. Catalyst.
CO₂RR. CO₂ Reduction Reaction.
CPE. Controlled Potential Electrolysis.
CV. Cyclic Voltammetry or Cyclic Voltammogram.
D. Doublet or deuterium.
DCM. Dichloromethane
DFT. Density Functional Theory.
DMF. Dimethylformamide.
DMPHEN. 2,8-dimethyl-1,10-phenanthroline.
DOSY. Diffusion Ordered Spectroscopy
D_x. Compound with x deuterium atoms.
E. Electron.
E°. Thermodynamic reduction or oxidation potential.
E_p. Peak reduction or oxidation potential.
EPR. Electron Paramagnetic Resonance.
EPR. Electron Paramagnetic Resonance.
Eqn. Equation.
Equiv. Equivalent(s).
ESI-MS. Electrospray Ionization-Mass Spectrometry.
FT. Fourier Transform.
g. Electron g-factor.
GC. Gas Chromatography.
HER. Hydrogen Evolution Reaction.
HOPG. Highly Ordered Pyrolytic Graphite.
HPLC. High-Performance Liquid Chromatography.
I. Nuclear spin quantum number.
ⁱPr. Isopropyl.
IR. Infrared.
J. NMR coupling constant.
L. Generic ligand or liter.
LTQ. Linear Trap Quadrupole.
Lut. 2,6-lutidine.
M. Multiplet or metal.

NMR. Nuclear Magnetic Resonance.
Nuc. Nucleophile.
OTf. Trifluoromethanesulfonate anion.
P₃^B. Tris(*o*-diisopropylphosphinophenyl)borane.
Phen. 1,10-phenanthroline.
^{py}P₃^B. (*o*-^{*i*}Pr₂P-*p*-O(CH₂)₄pyrene-(C₆H₄))₃B.
Pyrr. Pyrrolidinone.
Q. Stern-Volmer quenching fraction, quality factor, or quartet.
R. Alkyl or aryl group.
S. Siemen (Ω^{-1}).
S. Spin quantum number.
SCE. Saturated Calomel Electrode.
SET. Single Electron Transfer.
S_N2. Bimolecular nucleophilic substitution.
S_NAr. Nucleophilic aromatic substitution.
S_{RN}1. Unimolecular radical nucleophilic substitution.
T. Triplet.
t-Bu. Tertiary-butyl.
TD-DFT. Time-Dependent Density Functional Theory.
TEMPO. 1-hydroxyl-2,2,6,6-tetramethylpiperidine anion.
TEMPOH. 1-hydroxyl-2,2,6,6-tetramethylpiperidine.
TMS. Tetramethylsilane.
UV-vis. Ultraviolet-visible.
X-band. Radio frequency range from 8.0 to 12.0 GHz (typically ~9.5 GHz for EPR).
XPS. X-ray Photoelectron Spectroscopy.
 δ . NMR chemical shift.
 ϵ . Extinction coefficient.
 Λ_m . Molar conductivity.
 μ_B . Bohr Magneton.
 μ_{eff} . Effective magnetic moment.
 Φ . Quantum Yield.

INTRODUCTION

1.1 Motivation

Over the current century, rapidly growing world population and increased energy usage in the developing world is projected to lead to at least a three-fold increase of worldwide energy usage.¹ The majority of energy currently comes from non-renewable sources that produce CO₂ emissions, contributing to climate change.² While renewable energy alternatives exist for providing electricity with a low carbon footprint, many chemical processes are reliant on fossil-fuel feedstocks such as natural gas.³

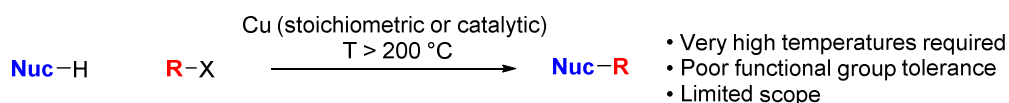
Furthermore, many important chemical processes rely on precious metals such as Pd, Rh, and Ir.^{4,5} These metals have low abundance on earth and their continued usage is not sustainable based on projected worldwide growth. Due to the use of precious metals and fossil-fuel based chemical feedstocks in many vital chemical processes, there is an urgent need to develop new chemical methods that use earth-abundant metals and incorporate alternative sources of energy such as sunlight and electricity.⁶

The use of alternative chemical processes opens up new methods for bond formation based on divergent reactivity.⁷ The development on new strategies for difficult bond formation reactions also opens up the possibility of discovering new transformations unachievable with previous methods. To better apply these new chemical methods to broader classes of reactions, we seek to understand the mechanism of these transformations and identify key reaction steps that we can alter through reaction design. The design and study

of photochemical and electrochemical reactions mediated by earth-abundant metals will lead to a greater understanding of reaction pathways operative in these classes of reactions.

However, many barriers exist to elucidating pathways of photochemical and electrochemical reactions. Photochemical reactions are often complex, and common spectroscopic methods that are suitable for thermally-driven reactions are not always applicable to their study. Electrochemical transformations can be difficult to control due to the interfacial and heterogeneous nature of electron transfer. Multi-electron, multi-proton redox processes are also complex due to the vast number of possible reaction pathways that can be spanned. Despite these difficulties, improvement and study of electrochemical and photochemical reactions is necessary to better employ renewable energy sources for chemical reactions. This thesis will discuss the study of photochemical bond formation reactions and development of an electrochemical N₂ reduction system.

1.2 Copper-Mediated Cross Coupling and Photochemistry



Scheme 1.1: Copper-mediated Ullmann coupling.

The coupling of nucleophiles and electrophiles catalyzed by copper dates back to the early 20th century, making it the first example of metal-catalyzed cross-coupling (Scheme 1.1).^{8,9} These early coupling reactions required harsh reaction conditions and showed limited functional group tolerance, leading to these methods being superseded by catalytic reactions based on precious metals such as palladium.¹⁰ In the early 21st century, it was discovered that the addition of chelating ligands, typically bidentate nitrogen donors, led to enhanced reactivity at lower temperatures with broader functional group tolerance relative to ligand-

free conditions (Scheme 1.2).¹¹ Over the last 15 years, there has been a significant growth in the use and number of reports of copper-catalyzed reactions.¹²



Scheme 1.2: Copper-catalyzed, ligand-accelerated Ullmann coupling.

Copper complexes have also been noted for their desirable photophysical properties, such as long excited-state lifetimes and highly reducing excited states.¹³ Our group has studied a number of P- and N-coordinated Cu^I complexes that access highly-reducing excited states, and we sought to employ these complexes to achieve copper-mediated bond formation reactions through single-electron redox processes.^{14–17} In 2012, we reported the copper-catalyzed coupling of carbazole with aryl halides through a radical pathway (Figure 1.1).¹⁸ This approach has been successfully expanded to a number of nucleophiles and electrophiles, yet many mechanistic questions remained (and still remain) unanswered.

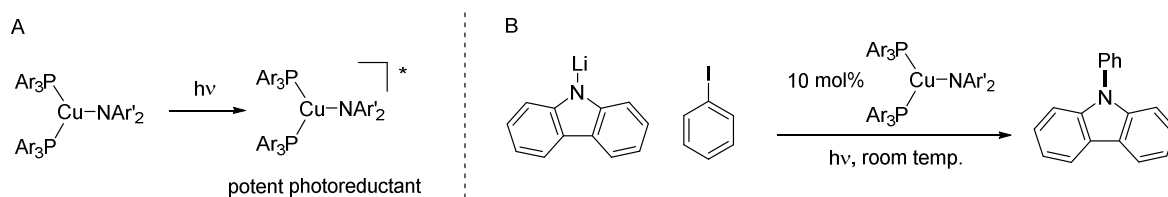


Figure 1.1: (A) Photoexcitation of a Cu^I-amide to access a highly reducing excited state. (B) Photoinduced C–N cross-coupling catalyzed by a Cu^I-amide.

1.3 Mechanism of Copper-mediated Coupling Reactions

Despite the long history of copper-catalyzed coupling reactions, very little was understood about the pathways operative in these reactions until recently. This lack of

understanding provided an obstacle to reaction discovery and optimization, as chemists were not able to make rational choices in testing substrates and ligands.

Early mechanistic work on thermal copper-catalyzed coupling reactions demonstrated that Cu^{I} -nucleophile complexes are key reaction intermediates, and that these intermediates can react with electrophiles.¹⁹ Several mechanisms have been proposed for this step, including (i) oxidative addition to generate a Cu^{III} intermediate, (ii) halogen atom transfer to generate a Cu^{II} -halide and electrophile radical, (iii) single-electron transfer (SET) to generate a Cu^{II} complex and electrophile radical, and (iv) σ -bond metathesis through a 4-centered transition state (Figure 1.2).

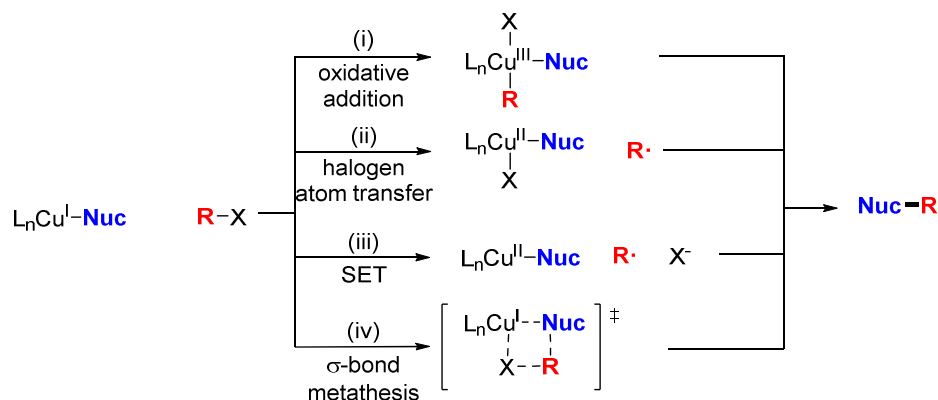


Figure 1.2: Possible pathways for ligand-accelerated Ullmann coupling reactions.

A number of radical clock and radical trapping experiments have disfavored mechanisms involving the formation of a free electrophile radical (Figure 1.3).^{19,20} However, these studies do not exclude the possibility of short-lived radical intermediates that undergo rapid recombination. Mechanistic studies on the reaction of iodobenzene and both methanol and methylamine concluded that both iodine atom transfer and single electron transfer mechanisms were accessible, with the preferred pathway depending on the nature of the nucleophile and ancillary ligand.²¹ While evidence exists for all pathways mentioned, most

proposals favor oxidative addition to generate a Cu^{III} species.²² The Ribas and Stahl groups demonstrated the viability of this oxidative addition mechanism by stoichiometrically demonstrating the synthesis of a macrocyclic Cu^{III} complex that undergoes reductive elimination to form a C–N bond (Scheme 1.3).²³ It is likely that different mechanisms may be operative in thermal Ullmann coupling reactions depending on the reaction conditions, or that multiple pathways may be accessible even in a single reaction.

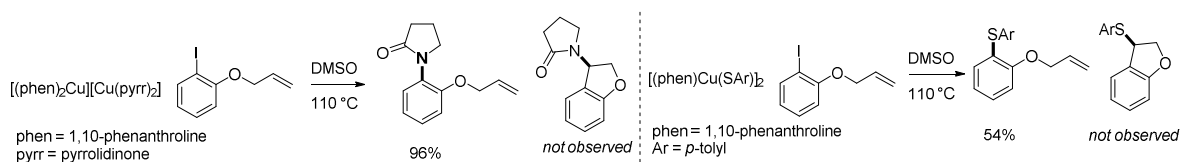
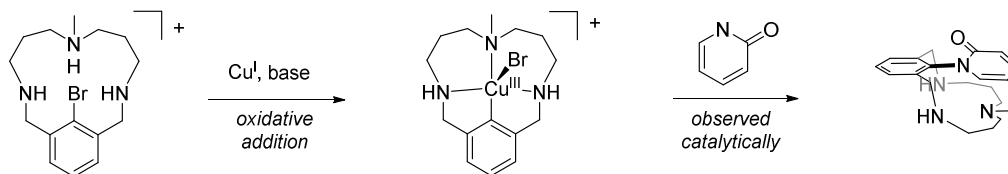


Figure 1.3: Radical clock experiments disfavoring the intermediacy of an aryl radical in the copper-catalyzed C–N (left) and C–S (right) coupling reactions.



Scheme 1.3: Model chemistry demonstrating the viability of a $\text{Cu}^{\text{I}}/\text{Cu}^{\text{III}}$ cycle based on oxidative addition and reductive elimination for C–N coupling.

In the photoinduced arylation of carbazole by a copper phosphine complex, early evidence supports a mechanism involving photoexcitation of a bis-phosphine copper carbazolid species as the first step.¹⁸ Complexes of this type can be quenched by iodobenzene, and EPR data of a frozen reaction mixture revealed the presence of a Cu^{II} species, consistent with photoinduced single-electron transfer (SET) from Cu^{I} to iodobenzene to form a Cu^{II} species and an aryl radical (Figure 1.4). Radical cyclization

experiments supported the intermediacy of an aryl radical, but the mechanism of the bond formation step was not determined.

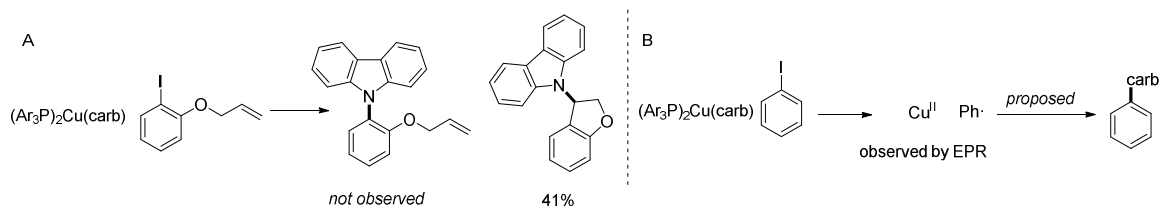


Figure 1.4: Early mechanistic studies of photoinduced, Cu-catalyzed cross-coupling. (A) Radical clock experiments demonstrating the intermediacy of an aryl radical. (B) Observation of a Cu^{II} species under catalytic conditions, which is proposed to be involved in C–N bond formation.

Following this report, a number of photoinduced copper-catalyzed cross coupling reactions were reported by our group, including N-alkylation,^{24, 25} S-arylation,²⁶ O-arylation,²⁷ and C-alkylation reactions.²⁸ These reactions did not require traditional ligands such as phosphines, and proceeded under varying conditions. We then sought to investigate the mechanism of these reactions to determine the factors affecting these ligand-free reactions and to characterize the mechanistic diversity of these reactions. In particular, we sought to determine the active species in these reactions, understand their photochemical properties, and better understand the nature of the coupling step.

1.4 Reduction of N_2 to NH_3 by Molecular Catalysts

The splitting of dinitrogen into ammonia is an essential process for worldwide agriculture, and is performed on a scale of 413 Tg N annually.²⁹ Nitrogen is fixed naturally primarily by nitrogenase enzymes that reside in root nodules of plants such as soybeans and

other legumes.³⁰ However, the amount of nitrogen fixed enzymatically falls significantly short of current worldwide demand.^{29,31}

As a supplement to natural sources of fixed nitrogen, industrial ammonia production represents a significant cost for the efficient growth of various crops. Industrially, N_2 is fixed by the Haber-Bosch process on a scale of 120 Tg N annually.³¹ The Haber-Bosch process employs an iron-based catalyst to convert H_2 and N_2 to ammonia at high temperature and pressure. While efficient, the Haber-Bosch process uses 2% of the global energy output and requires significant infrastructure. The majority of this energy input is employed for H_2 production through steam reforming and the water-gas shift reaction, which leads to CO_2 formation.^{29,32} The low volumetric energy density of H_2 also requires its on-site production and limits Haber-Bosch plants to areas that have large amounts of hydrocarbon fuels.³³ Development of scalable alternatives to the Haber-Bosch process that can be coupled to solar light or energy is important to the decentralized production of ammonia in the developing world, as well as to meeting the growing demand for ammonia-based fertilizer throughout the developed world.

As an alternative to the Haber-Bosch process, the fixation of N_2 with protons and electrons has been proposed as a scalable and energy-efficient method.³³ In particular, the reduction of dinitrogen with electricity derived from renewable sources is of particular interest. Significant progress has been made in the reduction of dinitrogen by transition metal

complexes over the past 50 years, although efficient catalytic reduction of N_2 remains difficult.

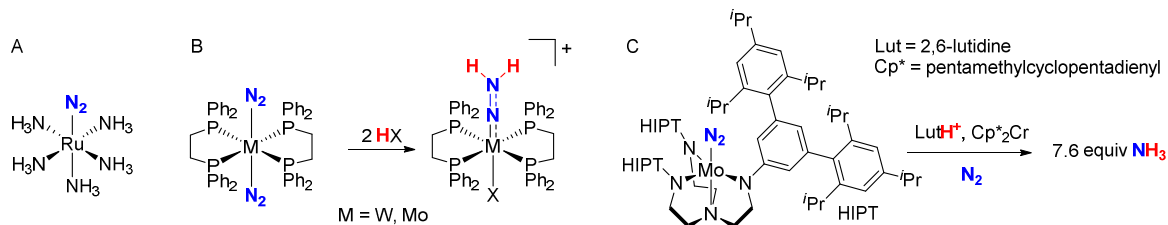


Figure 1.5: (A) The first example of N_2 binding to a transition metal. (B) Protonation of a metal-bound N_2 fragment to give N–H bond formation. (C) Catalytic reduction of N_2 to ammonia by a molybdenum complex.

The binding of N_2 to a transition metal center was first observed by Allen and Senoff at a Ru^{II} center in 1965.³⁴ In 1972, protonation of a metal-bound N_2 fragment was first reported by Chatt,³⁵ to give a $M=NNH_2$ species (Figures 1.5A, 1.5B). Catalytic reduction of N_2 to ammonia was then first reported by Schrock in 2003 at a Mo center (Figure 1.5C).³⁶ This report was followed by a number of other reports of catalytic N_2 reduction, including the reduction of N_2 to NH_3 by P_3^BFe by our group.^{37, 38} Despite the rapidly growing number

of reports of N₂ reduction by molecular complexes, chemical reductants and large driving forces are required in nearly every case.

1.4.1 Viability of Electrochemical Reduction

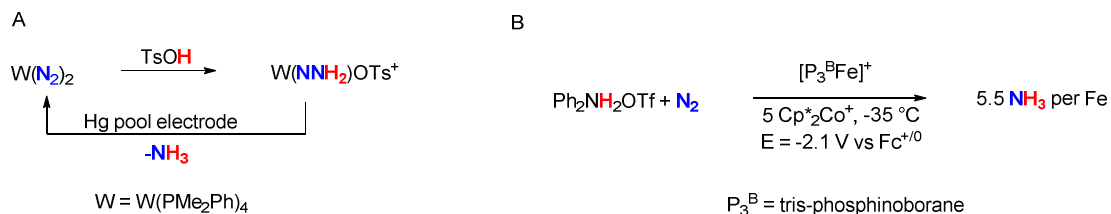


Figure 1.6: (A) Stoichiometric reduction of N₂ to ammonia by a tungsten complex at a Hg pool electrode by Pickett. (B) Electrocatalytic reduction of N₂ to ammonia by a molecular iron complex and a cocatalytic redox mediator by our group.

While most examples of molecular N₂ fixation have utilized relatively strong chemical reductants as the electron source, there has been long-standing interest in using alternative electron sources in N₂ fixation. Reduction of dinitrogen to ammonia without stoichiometric chemical reductants is necessary for coupling ammonia production to sunlight or electricity. In 1985, Pickett and coworkers demonstrated the stoichiometric reduction of N₂ to NH₃ at an electrode mediated by a tungsten phosphine complex (Figure 1.6A).^{39–41} Recently, our group has demonstrated the electrocatalytic reduction of N₂ at low temperature by a tris-phosphinoborane iron catalyst (P₃^BFe, Figure 1.6B).^{42, 43} This was followed by the Berben group's report of stoichiometric N₂ electroreduction by an aluminum complex at

lower overpotential.⁴⁴ These electroreductions demonstrate the viability of a molecular electrochemical strategy to reduce N_2 to ammonia.

1.5 Surface Attachment of Molecular Electrocatalysts

Electrocatalysis is fundamentally important for securing our energy future and producing chemical fuels from renewable energy.⁴⁵ Catalysis by synthetic transition metal complexes offer significant advantages over heterogeneous materials, including the ability to control interactions in their coordination sphere and the multitude of spectroscopic techniques available to study mechanism. These mechanistic understandings can allow rational alteration of catalysts to increase activity and stability.

A number of difficulties arise when soluble molecular complexes are employed as electrocatalysts in solution.⁴⁶ Only a small portion of the added catalyst is electrochemically active at a given time, deleterious bimolecular pathways can occur, catalyst can diffuse into both chambers of the electrochemical cell, and mechanistic study of molecular electrocatalysts presents numerous challenges. To avoid these difficulties, molecular catalysts can be immobilized on an electrode surface. While appealing, catalyst immobilization presents its own challenges. Most immobilization techniques require significant modification to the original catalyst synthesis, and may not be broadly applicable.

It is then difficult to determine the nature of the metal sites on the electrode, and the resulting catalyst activity may differ from that of the freely diffusing catalyst.

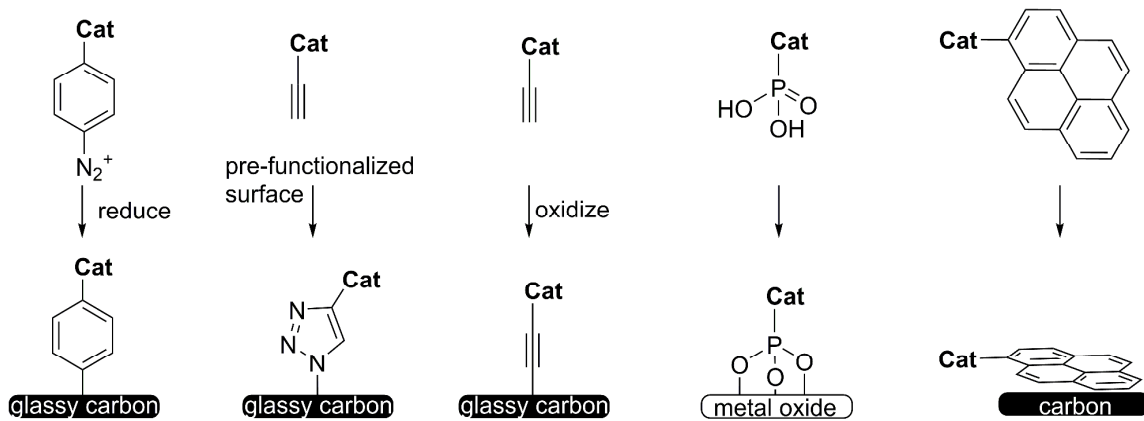


Figure 1.7: Overview of common strategies for surface attachment of molecular electrocatalysts.

Surface immobilization can be achieved by a number of approaches by using various types of catalyst-surface interactions, including both covalent and non-covalent attachment (Figure 1.7). Common covalent strategies include reduction of an aryl diazonium, Cu-catalyzed alkyne-azide click reaction, and alkyne oxidation. Common non-covalent strategies include adsorption of phosphonates on metal oxide layers and adsorption of pyrene moieties onto graphitic carbon surfaces. Covalent attachment methods generally require the incorporation of reactive functional groups and harsh redox processes that may interfere with catalyst synthesis, while adsorption on metal oxide layers allow limited electrode materials to be used.

A number of electrocatalytic reactions relevant to the generation of chemical fuels from electricity have been demonstrated by surface-attached molecular catalysts. The hydrogen evolution reaction (HER) has been heavily studied, as it is the simplest fuel-

forming reaction. A broad number of attachment strategies have been demonstrated for HER by an immobilized catalyst.⁴⁶ The CO₂ reduction reaction (CO₂RR) has also been explored; the harsher and more reducing conditions required for CO₂RR have however limited the applicability of many strategies. Adsorption of pyrene-containing catalysts has been most broadly successful,⁴⁷⁻⁵⁰ although other strategies have been successfully demonstrated.⁵¹⁻⁵⁷

1.6 Chapter Summaries

Chapter 2 discusses an in-depth mechanistic study of the photoinduced, copper-mediated cross-coupling of aryl thiols with aryl halides. In particular, I focus on the stoichiometric photochemistry and subsequent reactivity of a [Cu^I(SAr)₂]⁻ complex (Ar = 2,6-dimethylphenyl). A broad array of experimental techniques furnish data consistent with a pathway in which a photoexcited [Cu^I(SAr)₂]^{-*} complex undergoes SET to generate a Cu^{II} species and an aryl radical, which then couple through an in-cage radical recombination.

Chapter 3 discusses the surface attachment of a P₃^BFe complex to a carbon electrode, and the electrochemical generation of ammonia from N₂ by the surface-appended species. Synthetic modification of a previously-reported P₃^BFe complex by addition of three pyrene substituents onto the catalyst backbone allows non-covalent attachment onto a graphite surface. The resulting functionalized electrode shows good stability towards desorption under highly reducing conditions, and produces 1.4 equiv NH₃ per iron site. The data

presented provide the first demonstration of electrochemical nitrogen fixation by a molecular complex appended to an electrode.

1.7 References

- (1) Lewis, N. S.; Nocera, D. G. Powering the Planet: Chemical Challenges in Solar Energy Utilization. *Proc. Natl. Acad. Sci.* **2006**, *103* (43), 15729–15735.
- (2) Balzani, V.; Credi, A.; Venturi, M. Photochemical Conversion of Solar Energy. *ChemSusChem* **2008**, *1* (1–2), 26–58.
- (3) Olah, G. A. Beyond Oil and Gas: The Methanol Economy. *Angew. Chem. Int. Ed.* **2005**, *44* (18), 2636–2639.
- (4) J. Dunn, P. The Importance of Green Chemistry in Process Research and Development. *Chem. Soc. Rev.* **2012**, *41* (4), 1452–1461.
- (5) Torborg, C.; Beller, M. Recent Applications of Palladium-Catalyzed Coupling Reactions in the Pharmaceutical, Agrochemical, and Fine Chemical Industries. *Adv. Synth. Catal.* **2009**, *351* (18), 3027–3043.
- (6) Chirik, P.; Morris, R. Getting Down to Earth: The Renaissance of Catalysis with Abundant Metals. *Acc. Chem. Res.* **2015**, *48* (9), 2495–2495.
- (7) Holland, P. L. Distinctive Reaction Pathways at Base Metals in High-Spin Organometallic Catalysts. *Acc. Chem. Res.* **2015**, *48* (6), 1696–1702.
- (8) Ullmann, F.; Bielecki, J. Ueber Synthesen in Der Biphenylreihe. *Berichte Dtsch. Chem. Ges.* **1901**, *34* (2), 2174–2185.

- (9) Hassan, J.; Sévignon, M.; Gozzi, C.; Schulz, E.; Lemaire, M. Aryl–Aryl Bond Formation One Century after the Discovery of the Ullmann Reaction. *Chem. Rev.* **2002**, *102* (5), 1359–1470.
- (10) Johansson Seechurn, C. C. C.; Kitching, M. O.; Colacot, T. J.; Snieckus, V. Palladium-Catalyzed Cross-Coupling: A Historical Contextual Perspective to the 2010 Nobel Prize. *Angew. Chem. Int. Ed.* **2012**, *51* (21), 5062–5085.
- (11) Beletskaya, I. P.; Cheprakov, A. V. The Complementary Competitors: Palladium and Copper in C–N Cross-Coupling Reactions. *Organometallics* **2012**, *31* (22), 7753–7808.
- (12) Thapa, S.; Shrestha, B.; K. Gurung, S.; Giri, R. Copper-Catalysed Cross-Coupling: An Untapped Potential. *Org. Biomol. Chem.* **2015**, *13* (17), 4816–4827.
- (13) Horváth, O. Photochemistry of Copper(I) Complexes. *Coord. Chem. Rev.* **1994**, *135–136*, 303–324.
- (14) Harkins, S. B.; Peters, J. C. A Highly Emissive Cu₂N₂ Diamond Core Complex Supported by a [PNP][−] Ligand. *J. Am. Chem. Soc.* **2005**, *127* (7), 2030–2031.
- (15) Miller, A. J. M.; Dempsey, J. L.; Peters, J. C. Long-Lived and Efficient Emission from Mononuclear Amidophosphine Complexes of Copper. *Inorg. Chem.* **2007**, *46* (18), 7244–7246.
- (16) Lotito, K. J.; Peters, J. C. Efficient Luminescence from Easily Prepared Three-Coordinate Copper(I) Arylamidophosphines. *Chem. Commun.* **2010**, *46* (21), 3690–3692.

- (17) Deaton, J. C.; Switalski, S. C.; Kondakov, D. Y.; Young, R. H.; Pawlik, T. D.; Giesen, D. J.; Harkins, S. B.; Miller, A. J. M.; Mickenberg, S. F.; Peters, J. C. E-Type Delayed Fluorescence of a Phosphine-Supported $\text{Cu}_2(\mu\text{-NAr}_2)_2$ Diamond Core: Harvesting Singlet and Triplet Excitons in OLEDs. *J. Am. Chem. Soc.* **2010**, *132* (27), 9499–9508.
- (18) Creutz, S. E.; Lotito, K. J.; Fu, G. C.; Peters, J. C. Photoinduced Ullmann C–N Coupling: Demonstrating the Viability of a Radical Pathway. *Science* **2012**, *338* (6107), 647–651.
- (19) Tye, J. W.; Weng, Z.; Johns, A. M.; Incarvito, C. D.; Hartwig, J. F. Copper Complexes of Anionic Nitrogen Ligands in the Amidation and Imidation of Aryl Halides. *J. Am. Chem. Soc.* **2008**, *130* (30), 9971–9983.
- (20) Chen, C.; Weng, Z.; Hartwig, J. F. Synthesis of Copper(I) Thiolate Complexes in the Thioetherification of Aryl Halides. *Organometallics* **2012**, *31* (22), 8031–8037.
- (21) Jones, G. O.; Liu, P.; Houk, K. N.; Buchwald, S. L. Computational Explorations of Mechanisms and Ligand-Directed Selectivities of Copper-Catalyzed Ullmann-Type Reactions. *J. Am. Chem. Soc.* **2010**, *132* (17), 6205–6213.
- (22) Monnier, F.; Taillefer, M. Catalytic C–C, C–N, and C–O Ullmann-Type Coupling Reactions. *Angew. Chem. Int. Ed.* **2009**, *48* (38), 6954–6971.
- (23) Casitas, A.; King, A. E.; Parella, T.; Costas, M.; Stahl, S. S.; Ribas, X. Direct Observation of $\text{Cu}^{\text{I}}/\text{Cu}^{\text{III}}$ Redox Steps Relevant to Ullmann-Type Coupling Reactions. *Chem. Sci.* **2010**, *1* (3), 326–330.

- (24) Bissember, A. C.; Lundgren, R. J.; Creutz, S. E.; Peters, J. C.; Fu, G. C. Transition-Metal-Catalyzed Alkylations of Amines with Alkyl Halides: Photoinduced, Copper-Catalyzed Couplings of Carbazoles. *Angew. Chem. Int. Ed.* **2013**, *52* (19), 5129–5133.
- (25) Ziegler, D. T.; Choi, J.; Muñoz-Molina, J. M.; Bissember, A. C.; Peters, J. C.; Fu, G. C. A Versatile Approach to Ullmann C–N Couplings at Room Temperature: New Families of Nucleophiles and Electrophiles for Photoinduced, Copper-Catalyzed Processes. *J. Am. Chem. Soc.* **2013**, *135* (35), 13107–13112.
- (26) Uyeda, C.; Tan, Y.; Fu, G. C.; Peters, J. C. A New Family of Nucleophiles for Photoinduced, Copper-Catalyzed Cross-Couplings via Single-Electron Transfer: Reactions of Thiols with Aryl Halides Under Mild Conditions (0 °C). *J. Am. Chem. Soc.* **2013**, *135* (25), 9548–9552.
- (27) Tan, Y.; Muñoz-Molina, J. M.; Fu, G. C.; Peters, J. C. Oxygen Nucleophiles as Reaction Partners in Photoinduced, Copper-Catalyzed Cross-Couplings: O-Arylations of Phenols at Room Temperature. *Chem. Sci.* **2014**, *5* (7), 2831–2835.
- (28) Ratani, T. S.; Bachman, S.; Fu, G. C.; Peters, J. C. Photoinduced, Copper-Catalyzed Carbon–Carbon Bond Formation with Alkyl Electrophiles: Cyanation of Unactivated Secondary Alkyl Chlorides at Room Temperature. *J. Am. Chem. Soc.* **2015**, *137* (43), 13902–13907.
- (29) Fowler, David; Coyle, Mhairi; Skiba, Ute; Sutton, Mark A.; Cape, J. Neil; Reis, Stefan; Sheppard, Lucy J.; Jenkins, Alan; Grizzetti, Bruna; Galloway, James N.; et al. The Global Nitrogen Cycle in the Twenty-First Century. *Philos. Trans. R. Soc. B Biol. Sci.* **2013**, *368* (1621), 20130164.

- (30) Mus, F.; Crook, M. B.; Garcia, K.; Costas, A. G.; Geddes, B. A.; Kouri, E. D.; Paramasivan, P.; Ryu, M.-H.; Oldroyd, G. E. D.; Poole, P. S.; et al. Symbiotic Nitrogen Fixation and the Challenges to Its Extension to Nonlegumes. *Appl Env. Microbiol* **2016**, 82 (13), 3698–3710.
- (31) Erisman, J. W.; Sutton, M. A.; Galloway, J.; Klimont, Z.; Winiwarter, W. How a Century of Ammonia Synthesis Changed the World. *Nat. Geosci.* **2008**, 1, 636–639.
- (32) Recently, the possibility of producing ammonia from dihydrogen derived from water electrolysis has also been explored as a low-carbon alternative to steam reforming. However, this process is extremely energy intensive and relies on a non-abundant platinum catalyst.
- (33) Singh, V.; Dincer, I.; Rosen, M. A. Chapter 4.2 - Life Cycle Assessment of Ammonia Production Methods. In *Exergetic, Energetic and Environmental Dimensions*; Dincer, I., Colpan, C. O., Kizilkan, O., Eds.; Academic Press, 2018; pp 935–959.
- (34) Allen, A. D.; Senoff, C. V. Nitrogenopentammineruthenium(II) Complexes. *Chem. Commun. Lond.* **1965**, 0 (24), 621–622.
- (35) Chatt, J.; Heath, G. A.; Richards, R. L. The Reduction of Ligating Dinitrogen to Yield a Ligating N₂H₂ Moiety. *J. Chem. Soc. Chem. Commun.* **1972**, 0 (18), 1010–1011.
- (36) Yandulov, D. V.; Schrock, R. R. Catalytic Reduction of Dinitrogen to Ammonia at a Single Molybdenum Center. *Science* **2003**, 301 (5629), 76–78.
- (37) Anderson, J. S.; Rittle, J.; Peters, J. C. Catalytic Conversion of Nitrogen to Ammonia by an Iron Model Complex. *Nature* **2013**, 501 (7465), 84–87.
- (38) Roux, Y.; Duboc, C.; Gennari, M. Molecular Catalysts for N₂ Reduction: State of the Art, Mechanism, and Challenges. *ChemPhysChem* **2017**, 18 (19), 2606–2617.

- (39) Pickett, C. J.; Talarmin, J. Electrosynthesis of Ammonia. *Nature* **1985**, *317* (6038), 652.
- (40) Al-Salih, T. I.; Pickett, C. J. Electron-Transfer Reactions in Nitrogen Fixation. Part 1. The Electrosynthesis of Dinitrogen, Hydride, Isocyanide, and Carbonyl Complexes of Molybdenum: Intermediates, Mechanisms, and Energetics. *J. Chem. Soc. Dalton Trans.* **1985**, *6*, 1255–1264.
- (41) Pickett, C. J.; Ryder, K. S.; Talarmin, J. Electron-Transfer Reactions in Nitrogen Fixation. Part 2. The Electrosynthesis of Ammonia: Identification and Estimation of Products. *J. Chem. Soc. Dalton Trans.* **1986**, *7*, 1453–1457.
- (42) Chalkley, M. J.; Del Castillo, T. J.; Matson, B. D.; Roddy, J. P.; Peters, J. C. Catalytic N₂-to-NH₃ Conversion by Fe at Lower Driving Force: A Proposed Role for Metallocene-Mediated PCET. *ACS Cent. Sci.* **2017**, *3* (3), 217–223.
- (43) Chalkley, M. J.; Del Castillo, T. J.; Matson, B. D.; Peters, J. C. Fe-Mediated Nitrogen Fixation with a Metallocene Mediator: Exploring pK_a Effects and Demonstrating Electrocatalysis. *J. Am. Chem. Soc.* **2018**, *140* (19), 6122–6129.
- (44) Sherbow, T. J.; Thompson, E. J.; Arnold, A.; Sayler, R. I.; Britt, R. D.; Berben, L. A. Electrochemical Reduction of N₂ to NH₃ at Low Potential by a Molecular Aluminum Complex. *Chem. – Eur. J.* **2019**, *25* (2), 454–458.
- (45) Markovic, N. M. Electrocatalysis: Interfacing Electrochemistry. *Nat. Mater.* **2013**, *12* (2), 101–102.
- (46) Bullock, R. M.; Das, A. K.; Appel, A. M. Surface Immobilization of Molecular Electrocatalysts for Energy Conversion. *Chem. – Eur. J.* **2017**, *23* (32), 7626–7641.

- (47) Axet, M. R.; Dechy-Cabaret, O.; Durand, J.; Gouygou, M.; Serp, P. Coordination Chemistry on Carbon Surfaces. *Coord. Chem. Rev.* **2016**, *308*, 236–345..
- (48) Kang, P.; Zhang, S.; Meyer, T. J.; Brookhart, M. Rapid Selective Electrocatalytic Reduction of Carbon Dioxide to Formate by an Iridium Pincer Catalyst Immobilized on Carbon Nanotube Electrodes. *Angew. Chem. Int. Ed.* **2014**, *53* (33), 8709–8713.
- (49) Maurin, A.; Robert, M. Noncovalent Immobilization of a Molecular Iron-Based Electrocatalyst on Carbon Electrodes for Selective, Efficient CO₂-to-CO Conversion in Water. *J. Am. Chem. Soc.* **2016**, *138* (8), 2492–2495.
- (50) Blakemore, J. D.; Gupta, A.; Warren, J. J.; Brunschwig, B. S.; Gray, H. B. Noncovalent Immobilization of Electrocatalysts on Carbon Electrodes for Fuel Production. *J. Am. Chem. Soc.* **2013**, *135* (49), 18288–18291.
- (51) Rosser, T. E.; Windle, C. D.; Reisner, E. Electrocatalytic and Solar-Driven CO₂ Reduction to CO with a Molecular Manganese Catalyst Immobilized on Mesoporous TiO₂. *Angew. Chem. Int. Ed.* **2016**, *55* (26), 7388–7392.
- (52) Yao, S. A.; Ruther, R. E.; Zhang, L.; Franking, R. A.; Hamers, R. J.; Berry, J. F. Covalent Attachment of Catalyst Molecules to Conductive Diamond: CO₂ Reduction Using “Smart” Electrodes. *J. Am. Chem. Soc.* **2012**, *134* (38), 15632–15635.
- (53) Kramer, W. W.; McCrory, C. C. L. Polymer Coordination Promotes Selective CO₂ Reduction by Cobalt Phthalocyanine. *Chem. Sci.* **2016**, *7* (4), 2506–2515.
- (54) Goff, A. L.; Artero, V.; Jusselme, B.; Tran, P. D.; Guillet, N.; Métafé, R.; Fihri, A.; Palacin, S.; Fontecave, M. From Hydrogenases to Noble Metal-Free Catalytic Nanomaterials for H₂ Production and Uptake. *Science* **2009**, *326* (5958), 1384–1387.

- (55) Rodriguez-Maciá, P.; Dutta, A.; Lubitz, W.; Shaw, W. J.; Rüdiger, O. Direct Comparison of the Performance of a Bio-Inspired Synthetic Nickel Catalyst and a [NiFe]-Hydrogenase, Both Covalently Attached to Electrodes. *Angew. Chem. Int. Ed.* **2015**, *54* (42), 12303–12307.
- (56) Zhanaidarova, A.; Moore, C. E.; Gembicky, M.; Kubiak, C. P. Covalent Attachment of [Ni(Alkynyl-Cyclam)]²⁺ Catalysts to Glassy Carbon Electrodes. *Chem. Commun.* **2018**, *54* (33), 4116–4119.
- (57) Zhanaidarova, A.; Ostericher, A. L.; Miller, C. J.; Jones, S. C.; Kubiak, C. P. Selective Reduction of CO₂ to CO by a Molecular Re(Ethynyl-Bpy)(CO)₃Cl Catalyst and Attachment to Carbon Electrode Surfaces. *Organometallics* **2019**, *38* (6), 1204–1207.